Journal of proteome research

Article

pubs.acs.org/jpr

Gut Microbiota Modulation Attenuated the Hypolipidemic Effect of Simvastatin in High-Fat/Cholesterol-Diet Fed Mice

Xuyun He,[†,#] Ningning Zheng,[†,#] Jiaojiao He,[†,#] Can Liu,[‡] Jing Feng,[‡] Wei Jia,[*,§,∥] and Houkai Li[*,†]

[†]Center for Chinese Medical Therapy and Systems Biology, Shanghai University of Traditional Chinese Medicine, Shanghai 201203, China

[‡]Laboratory Medicine of Southern Medical University Affiliated Fengxian Hospital, Shanghai 201499, China

[§]Center for Translational Medicine, and Shanghai Key Laboratory of Diabetes Mellitus, Shanghai Jiao Tong University Affiliated Sixth People's Hospital, Shanghai 200233, China

[∥]Cancer Epidemiology Program, University of Hawaii Cancer Center, Honolulu, Hawaii 96813, United States

Supporting Information

ABSTRACT: The hypolipidemic effect of simvastatin varies greatly among patients. In the current study, we investigated the gut microbial-involved mechanisms underlying the different responses to simvastatin. Male C57BL/6J mice were divided into control (Con), high-fat/cholesterol diet (HFD), antibiotic (AB), simvastatin (SV) and antibiotic_simvastatin (AB_SV) groups, respectively. At the end of the experiment, serum samples were collected for lipids and metabolomic analysis, and liver tissues for histology, gene and protein expression analysis. The results showed that antibiotic treatment not only altered the composition of gut microbiota, but attenuated the hypolipidemic effect of SV. A total of 16 differential metabolites between SV and HFD groups were identified with metabolomics, while most of them showed no statistical differences between AB_SV and HFD groups, and similar changes were also observed in bile acids profile. The expressions of several genes and proteins involved in regulating bile acids synthesis were significantly reversed by SV, but not AB_SV in HFD fed mice. In summary, our current study indicated that the hypolipidemic effect of SV was correlated with the composition of the gut microbiota, and the attenuated hypolipidemic effect of SV by gut microbiota modulation was associated with a suppression of bile acids synthesis from cholesterol.

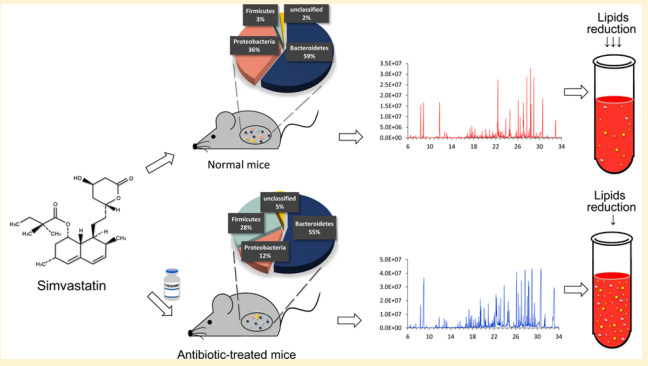

KEYWORDS: *simvastatin, hypolipidemic effect, antibiotic, gut microbiota, metabolomics*

INTRODUCTION

Simvastatin (SV) is one of the most widely used statins for reducing low density lipoprotein-cholesterol (LDL-c) and preventing cardiovascular disease by inhibiting 3-hydroxy-3-methyl glutaryl coenzyme A (HMG-CoA) reductase.[1−3] In the clinic, obvious variations in therapeutic benefits and LDL-c reduction upon SV therapy have been observed among patients, in which some "good" responders showed over 60%, whereas "poor" responders only had less than 10% reduction in LDL-c.[4] However, the mechanisms underlying the interindividual variation in the efficacy of SV are poorly known. Kaddurah-Daouk et al. conducted a series of investigations for deciphering the metabolic association with efficacy of SV between "good" and "poor" responders by using a metabolomic approach.[5,6] They found that several panels of metabolites were differently altered between "good" and "poor" responders upon SV therapy such as lipids, fatty acids, amino acids and gut microbiota-derived secondary bile acids. Moreover, they observed a strong correlation between the degree of LDL reduction and baseline levels of several secondary bile acids, including lithocholic acid (LCA), taurolithocholic acid (TLCA) and glycolithocholic acid (GLCA) which are produced by gut microbiota.[7] In addition, the different responses to SV therapy are also associated with higher baseline levels of coprostanol in patients, which is derived from the hydroxylation of cholesterol by gut microbiota.[7] Accordingly, the evidence highlights the involvement of gut microbiota in affecting individual responses to SV.

It has been well recognized that the gut microbiota plays critical roles in the development of various diseases,[8] as well as influencing both the pharmacokinetics and pharmacodynamics of many drugs.[9,10] In vitro experiments coupled with metabolomics indicated that SV is degraded into various metabolites by human intestinal microbiota,[11] while a similar study uncovered that the biotransformation of orally administered lovastatin could be altered in antibiotic-treated rats compared to normal rats.[12] As a result, we speculated that the

Received: November 15, 2016
Published: April 5, 2017

DOI: 10.1021/acs.jproteome.6b00984
J. Proteome Res. 2017, 16, 1900−1910

different responses toward SV therapy were due to differences in gut microbiota.

In the current study, we compared the hypolipidemic effect of SV in high-fat/cholesterol-diet fed mice with or without antibiotic TIENAM (Imipenem:Cilastatin Sodium = 1:1, 100 mg/kg) treatment orally, as well as their metabolic impacts and expression of genes involved in the cholesterol metabolism pathway in the liver. Our results demonstrated gut microbiota modulation with antibiotic treatment could attenuate the hypolipidemic effect of SV. Moreover, gut microbiota modulation resulted in obvious alterations of serum metabolic profiles in SV-treated mice including a panel of phospholipids and bile acids, as well as the expression of hepatic Cyp7a1 and Cyp7b1 genes and their protein levels. Our current results indicated that the different responses to SV therapy were, at least in part, due to the variation of gut microbiota composition.

MATERIALS AND METHODS

Chemicals

Simvastatin (SV) was purchased from MSD Pharmaceutical Company Limited (Hangzhou, China). TIENAM (Imipenem:-Cilastatin Sodium = 1:1) was obtained from Merck Sharp & Dohme Corp. All the primary and secondary antibodies for the Western blot analysis were purchased from Cell Signaling Technology (USA). TRIzol reagent used for total RNA extraction was purchased from Sigma-Aldrich (USA). High capacity cDNA reverse transcription kit and SYBR Master Mix were purchased from Applied Biosystems (USA); RIPA Lysis Buffer was purchased from Beyotime company (China). SuperSignal West Pico Chemiluminescent Subatrate was purchased from Thermo Fisher Scientific (USA). The derivatization reagent for GC−MS analysis, *N*,*O*-Bis-(trimethylsilyl)trifluoroacetamide (BSTFA) with 1% trimethylchlorosilane (TMCS) was purchased from Regis (Morton Grove,IL, USA).

Animal Experiments

Sixty male C57BL/6J mice (4-week-old) were purchased from Shanghai Laboratory Animal Center (Shanghai, China) and housed in a light-controlled room kept at a temperature of 23 ± 3 °C and a relative humidity of 50 ± 5% with free access to water and a normal standard chow diet. All the mice were acclimatized for 1 week prior to the experiments. Seven mice were randomly selected and fed with normal chow diet as the control group (Con, n = 7), while the rest 53 mice were fed with high-fat/cholesterol-diet (HFD) for 8 weeks. Then, the mice were divided into four groups as follows: HFD group (HFD, n = 8), antibiotic-treated group (AB, n = 10), simvastatin-treated group (SV, n = 13) and combined antibiotic and simvastatin treatment group (AB_SV, n = 12). The mice in AB and AB_SV groups were orally administrated with TIENAM (100 mg/kg) once a day during experiment according to the reference.[13] The mice in SV and AB_SV groups were treated with SV (20 mg/kg·day) by gavage. After another 4 weeks treatment, all the animals were sacrificed and the samples were collected and stored at −80 °C for subsequent analysis.

Analysis of Serum Lipids and Liver Histology

The serum total cholesterol (TC), triglyceride (TG), LDL and high density lipoprotein (HDL) were analyzed with enzymatic assay kits according the manufacturer's instructions. For liver histological analysis, the liver tissue was first fixed in 10% (volume/volume) formaldehyde, embedded in paraffin, and stained with hematoxylin-eosin (HE) according to the standard protocols.

Cecal DNA Extraction and Gut Microbiota Analysis

Cecal samples were collected from cecum of mice during sacrifice and frozen at −80 °C until use. Bacterial genomic DNA was extracted with 100 mg fecal samples using a fast DNA stool mini kit (QIAGEN, Germany) following the manufacturer's instructions. The extracted DNA samples were used as template for amplification of the V3 region of 16S rRNA gene. The PCR amplification, pyrosequencing of PCR amplicons and quality control were performed on Ion PGM System according to previously published methods.[14] The acquired valid and representative sequences of each sample were compared Greengenes database using the nearest alignment space termination algorithm,[15] and constructed a neighbor-joining tree with ARB.[16] Operational taxonomic units (OTUs) were delineated at 97% similarity level with Mothur software. The representative sequence of each OTU was selected with the most abundance and subjected to RDP classifier for taxonomical assignment with a bootstrap cutoff of 60%.[17,18] Alpha diversity was assessed with Rarefaction analysis and the Shannon−Wiener index with QIIME.[19] Weighted Fast UniFrac principal coordinate analysis (PCoA) was performed with the phylogenetic tree constructed by each OTU generated with QIIME.[19] The comparisons of bacteria abundance at phylum level between groups were performed with one-way ANOVA test after the normality analysis of all data.

Serum Metabolic Profiling with GC−MS and UPLC-QTOF-MS

Serum samples stored at −80 °C were thawed and vortexed for 5 s at room temperature and transferred. To a tube containing 10 μL of internal standard (0.1 mg/mL dulcitol), 30 μL serum sample was added and vortexed for 5 s. Subsequently, 120 μL of ice-cold methanol/chloroform (3:1) was added, the resulting mixture was vortexed for 30 s and placed at −20 °C for 20 min before centrifugation at 16000*g* and 4 °C for 15 min. Quality control (QC) sample pooled from representative serum samples of mice in every group were prepared and analyzed with the same procedure as that for the experiment samples in each batch. The supernatant was utilized for metabolic profiling with GC−MS and UPLC-QTOF-MS, respectively. The process of instrumental analysis and data preprocessing was described as the following:

GC−MS Analysis and Data Preprocessing

One vial containing 90 μL of supernatant of each sample was dried under a gentle nitrogen stream, and 30 μL of 20 mg/mL methoxylamine hydrochloride in pyridine was subsequently added. The resultant mixture was vortexed vigorously for 30 s and incubated at 37 °C for 90 min. Thirty microliters of BSTFA (with 1% TMCS) was added into the mixture, which was derivatized at 70 °C for 60 min prior to injection. At the same time, a blank derivatization sample (using deionized water instead of serum sample) was prepared in order to remove the background noise produced during sample preparation and GC−MS analysis. The derivatized serum samples were analyzed on an Agilent 7890A gas chromatography system coupled to an Agilent 5975C MSD system with inert Triple-Axis Detector (Agilent, CA). A HP-5MS fused-silica capillary column (30 m × 0.25 mm × 0.25 μm, Agilent J&W Scientific, Folsom, CA,

DOI: 10.1021/acs.jproteome.6b00984
J. Proteome Res. 2017, 16, 1900−1910

USA) was utilized to separate the derivatives. Helium was used as the carrier gas at a constant flow rate of 1 mL/min through the column. The injection volume was 1 μL, and the solvent delay time was 5 min. The initial oven temperature was held at 80 °C for 2 min, ramped to 300 °C at a rate of 10 °C/min, and finally held at 300 °C for 6 min. The temperature of the injector, transfer line, and ion source (electron impact) was set to 250, 290, and 230 °C, respectively. The collision energy was 70 eV. Mass data was acquired in a full-scan mode (m/z 50−600). The samples were analyzed in a random sequence.

The peak picking, alignment, deconvolution, and further processing of raw GC−MS data were performed according to previously published protocols.[20] The final data was exported as a peak table file, including observations (sample name), variables (rt_mz), and peak abundances. The data was normalized against total peak abundances before performing univariate and multivariate statistics.

UPLC-QTOF-MS Analysis and Data Preprocessing

Another one tube containing 10 μL supernatant from each sample was dried and reconstituted in 100 μL acetonitrile/water (1:1, v/v) containing 1 μg/mL L-phenylalanine-13C9,15N as internal standard prior to UPLC-QTOF-MS analysis. Chromatographic separation was performed on a Waters Acquity UPLC system with a BEH C18 column (2.1 mm × 100 mm, 1.7 μm) at a flow rate of 0.4 mL/min and 50 °C column temperature. The injection volume was 2 μL. The mobile phases consisted of water (phase A) and methanol (phase B), both with 0.1% formic acid (v/v). A linear gradient elution was performed with the following program: 0−0.5 min, 1% B; 1.5 min, 40% B; 5 min, 80% B; 9.3 min, 100% B; 12 min, 100% B; 12.01 min, 1% B and held to 14 min.

The eluents were analyzed on a hybrid quadrupole time-of-light mass spectrometer (Triple TOF 4600 system, AB Sciex, Comcord, ON, Canada) equipped with a DuoSpray ion source in positive ion mode. The pressures of nebulizer gas (GS1), heater gas (GS2) and curtain gas (CUR) were set to 50, 50, and 45 psi, respectively. Ionization voltage was set to 5000 V and spray temperature was 550 °C. A typical information dependent acquisition comprising the acquisition of a survey TOF MS spectrum and then a MS/MS experiment was applied in the analysis. The TOF MS scan was operated under the high resolution settings with a range of 50−1000 m/z and an accumulation time of 250 ms. The declustering potential (DP) and collision energy (CE) were set at 60 V and 10 eV, respectively, in the positive ion mode. In the second experiment, up to 10 candidate precursors per scan cycle were fragmented in collision-induced dissociation (CID) by a CE setting at 45 ± 15 eV, and the data were collected at a range of 50−1000 m/z with 10 ms accumulation time for the products of each precursor. The software for controlling instrument and collecting data was Analyst TF 1.6 (AB Sciex, Comcord, ON, Canada).

The raw data of UPLC-QTOF-MS were transformed to mzXML format (ProteoWizard) and then processed by XCMS and CAMERA packages in R software platform. In XCMS package, the peak picking (method = centWave, ppm = 15, peakwidth = c (5, 20), snthresh = 10), alignment (bw = 6 and 3 for the first and second grouping, respectively), and retention time correction (method = obiwarp) were conducted. In CAMERA package, the annotations of isotope peak, adducts, and fragments were performed with default parameters. The final data was exported as a peak table file, including observations (sample name), variables (rt_mz), and peak abundances. The data was normalized against total peak abundances before performing univariate and multivariate statistics.

Statistical Analysis and Identification of Differential Variables

For univariate statistical analysis of all acquired data between groups, the data were tested for normality first. The unnormalized data were log transformed and tested again to verify whether the transformed data were normally distributed. Then, the normally distributed data would be analyzed with one-way ANOVA followed by a posthoc test.

For multivariate statistical analysis of metabolomic data, the normalized data from GC−MS and UPLC-QTOF-MS were imported to Simca-P software (version 11.0), where the data were preprocessed by UV scaling and mean centering before performing PCA, and PLS-DA. The model quality is described by the R2X or R2Y and Q2 values. R2X (PCA) or R2Y (PLS-DA) is defined as the proportion of variance in the data explained by the models and indicates the goodness of fit. Q2 is defined as the proportion of variance in the data predictable by the model and indicates the predictability of the current model, calculated by cross-validation procedure. In order to avoid model overfitting, a default 7-round cross-validation in Simca-P software was performed throughout to determine the optimal number of principal components. The variables with VIP > 1 values of PLS-DA model and $P < 0.05$ values of univariate statistical analysis were identified as potential differential metabolites. Fold change was calculated as with the normalized peak intensity.

Metabolites Identification

For GC−MS data, the AMDIS software was applied to deconvolute mass spectra from raw GC−MS data, and the purified mass spectra were automatically matched with an in-house standard library including retention time and mass spectra, the Golm Metabolome Database, and the Agilent Fiehn GC−MS Metabolomics RTL Library (matching similarity larger than 70%). For UPLC-QTOF-MS data, the accurate m/z of precursors and product ions were matched against Metlin, MassBank, LipidBlast databases and an in-house standard library including retention time, accurate precursors, and product ions.

Analysis of Serum Bile Acids with UPLC−MS/MS

Ten μL of isotope labeled internal standards (125 ng/mL in 50% aqueous methanol) and 90 μL of methanol/acetonitrile (5:3, v/v) were added to 25 μL of thawed serum sample. The mixture was vortexed for 1 min and placed at 4 °C for 30 min prior to centrifugation at 16000g for 15 min (4 °C). The supernatant was dried under nitrogen stream and reconstituted in 50 μL of aqueous methanol (v/v). The redissolved solution was vortexed for 2 min and centrifuged at 16000g for 15 min (4 °C). The supernatant was used for detecting serum bile acids with UPLC−MS/MS. Chromatographic separation was performed on an Agilent Poroshell 120 SB-C18 column (2.7 μm, 2.1 mm × 50 mm) with a flow of 0.4 mL/min and 40 °C column temperature. The mobile phases consisted of water (phase A) and methanol (phase B), both with 10 mM ammonium acetate and 0.012% formic acid (v/v). A linear gradient elution was used with the following program: 0−0.5 min, 35% B; 2.5 min, 65% B; 6.7 min, 80% B; 6.71 min, 100% B; 8 min, 100% B; 8.01 min, 35% B and held to 10 min. The

DOI: 10.1021/acs.jproteome.6b00984
J. Proteome Res. 2017, 16, 1900−1910

eluents were detected by an AB Sciex TripleQuad 5500 (Comcord, ON, Canada) equipped with electrospray ionization (ESI) source in negative ion mode. The pressures of nebulizer gas (GS1), heater gas (GS2), curtain gas (CUR), and collision gas (CAD) were set to 50, 50, 30, and 8 psi, respectively. Ionization voltage was set to −4500 V and spray temperature was 550 °C. The precursors were fragmented and monitored in Multiple Reaction Monitoring (MRM) mode. The dwelling time was 10 ms for all transitions. The raw data were processed in Analyst 1.5.2 (AB Sciex, Comcord, ON, Canada). The relative quantification was obtained by normalized the peak area against internal standard (Cholic acid-D4).

Hepatic Gene Expression Analysis with RT^2 Profiler PCR Array

To test the hepatic gene expression involved in the cholesterol metabolism pathway, commercial RT^2 Profiler PCR Arrays were used for quantitation of 84 targeted genes involved in the cholesterol metabolism pathway (Cat no. PAHS-080Z, QIAGEN, Germany). Briefly, the total RNA was extracted with RNeasy Mini Kit (Cat no. 74104, QIAGEN, Germany) and 1 μg of total RNA was subjected to first strand cDNA synthesis with RT^2 HT First Strand Kit (Cat no. 330411, QIAGEN, Germany) according to the manufacturer's instructions. The synthesized cDNA samples were analyzed with RT^2 Profiler PCR Arrays in triplicate on Biorad Connect (Biorad, USA).

Western Blot

The expression of several hepatic proteins was analyzed with Western blot. Briefly, the total proteins were extracted from about 20 mg liver tissues with 500 μL of RIPA Lysis Buffer (Beyotime, China) according to well-established protocols. The protein concentrations were determined with Pierce Coomassie Protein Assay kit (Thermo Scientific). A total of 20 μg protein was loaded into each lane and separated by 10% SDS-PAGE gel, and then transferred to a PVDF membrane (Biorad, USA). The membrane was then blocked with 10% milk at room temperature. The membranes were incubated with primary antibodies (1:1000 dilution, Cell Signaling Technology, USA) overnight at 4 °C. Then, the membranes were washed with TBST (20 mM Tris-HCL, 137 mM NaCl, and 0.1% Tween20, pH7.5) three times at 10 min interval. The HRP-conjugated secondary antibodies were then incubated for 1h at room temperature. The membranes were exposed with SuperSignal West Pico Chemiluminescent Subatrate (Thermo Fisher Scientific, USA) and the resulting bands were quantified by using Amersham Imager 600 system (General Electric Company, USA). GAPDH was used as a control.

RESULTS

Antibiotic Treatment Attenuated the Hypolipidemic Effect of SV in Mice

To test whether the differential responses to SV treatment were associated with differences in the gut microbiota, mice were treated with SV for 8 weeks with or without AB intervention. The serum levels of TC, LDL, HDL and TG were significantly elevated in both HFD and AB groups indicating that AB did not affect the lipids metabolism per se. SV treatment significantly reduced the levels of TC, LDL, and HDL, while the combined administration of AB attenuated the hypolipidemic effect of SV (Figure 1), indicating that the hypolipidemic effect of SV was affected by antibiotic treatment.

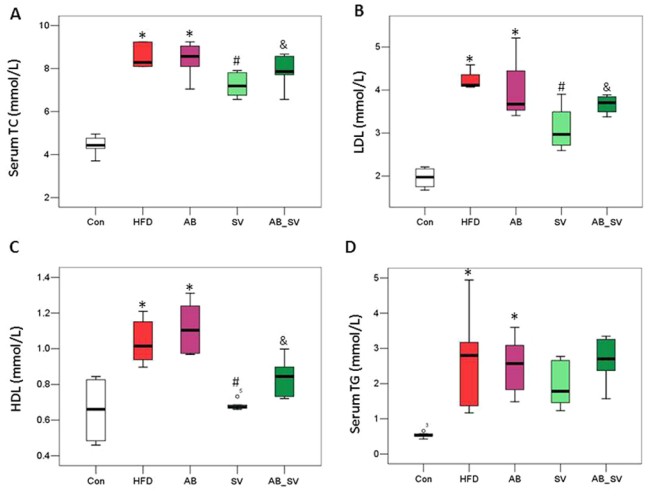

Figure 1. Antibiotic treatment attenuated the hypolipidemic effect of SV. (A–D) Serum TC, LDL, HDL and TG levels among groups. *P < 0.05 vs Con group; $^{\#}P$ < 0.05 vs HFD group; $^{\&}P$ < 0.05 vs SV group. Data are mean ± SD. Comparisons between groups were analyzed with one-way ANOVA followed by a posthoc test. Con: control group; HFD: high-fat/cholesterol diet group; AB: antibiotic group; SV: simvastatin (20 mg/kg) group; AB_SV: simvastatin (20 mg/kg) in the presence of antibiotic treatment.

Antibiotic Treatment Altered the Composition of Gut Microbiota

We next detected the compositional changes of gut microbiota by AB administration by using pyrosequencing on the V3 region of 16S rDNA of bacteria. A total of 263 732 valid reads were obtained from 22 fecal samples after normalization to the sample with minimal number of valid reads.On average each sample had 11 987 ± 55 reads for following analysis. Then, OTUs were binned with acquired valid reads at 97% similarity level against the Greengene database.[15] The Rarefaction and Shannon–Wiener curves showed that most of the diversities of bacteria in samples have been covered in the current sequencing depth (data not shown). A total of 39 966 OTUs were used for phyla analysis with RDP classifier at a bootstrap cutoff of 60%. The most abundant phyla included Bacteroidetes (21 108 OTUs, contributing 52.81% of all OTUs), Firmicutes (9042 OTUs, contributing 22.62% of all OTUs), Proteobacteria (7732 OTUs, contributing 19.35% of all OTUs) and Actinobacteria (82 OTUs, contributing 0.21% of all OTUs). Then, PCoA was performed to compare the differences of OTUs abundance among the five groups. Samples from AB and AB_SV groups were distinctly separated from Con, HFD and SV groups along the PC1 (42.79%), which accounted for the largest proportion of total variation (Figure 2A). Thus, the composition of the gut microbiota in both AB and AB_SV groups were distinctly different with that in another three groups at phylum level (Figure 2B). Further comparisons of bacteria abundance of the three major phyla were performed among groups including Bacteroidetes, Firmicutes, and Proteobacteria. There were no significant differences at the three major phyla between HFD and Con groups. However, dramatic reduction in abundance of Firmicutes, and increase in Proteobacteria was observed in both the AB and AB_SV groups, whereas abundance of Bacteroidetes was only significantly reduced in AB_SV group compared to HFD or SV group (Figure 2C). Therefore, AB administration altered the composition of the gut microbiota.

DOI: 10.1021/acs.jproteome.6b00984
J. Proteome Res. 2017, 16, 1900–1910

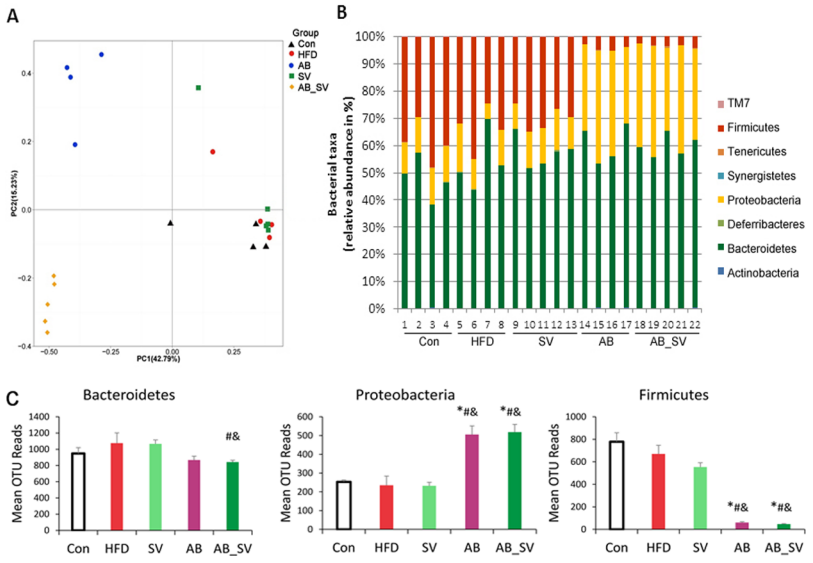

Figure 2. Antibiotic treatment altered the composition of the gut microbiota. (A) Weighted UniFrac PCoA plot based on OTU abundance of each mouse. Each point in the plot represents the gut microbiota of one mouse. (B) The relative taxonomic abundance at the phylum level of gut microbiota among groups. (C) The mean OUT reads of major phylum of gut microbiota among groups. *P < 0.05 vs Con group; $^{\#}P$ < 0.05 vs HFD group; $^{\&}P$ < 0.05 vs SV group. Comparisons between groups were analyzed with one-way ANOVA followed by a posthoc test.

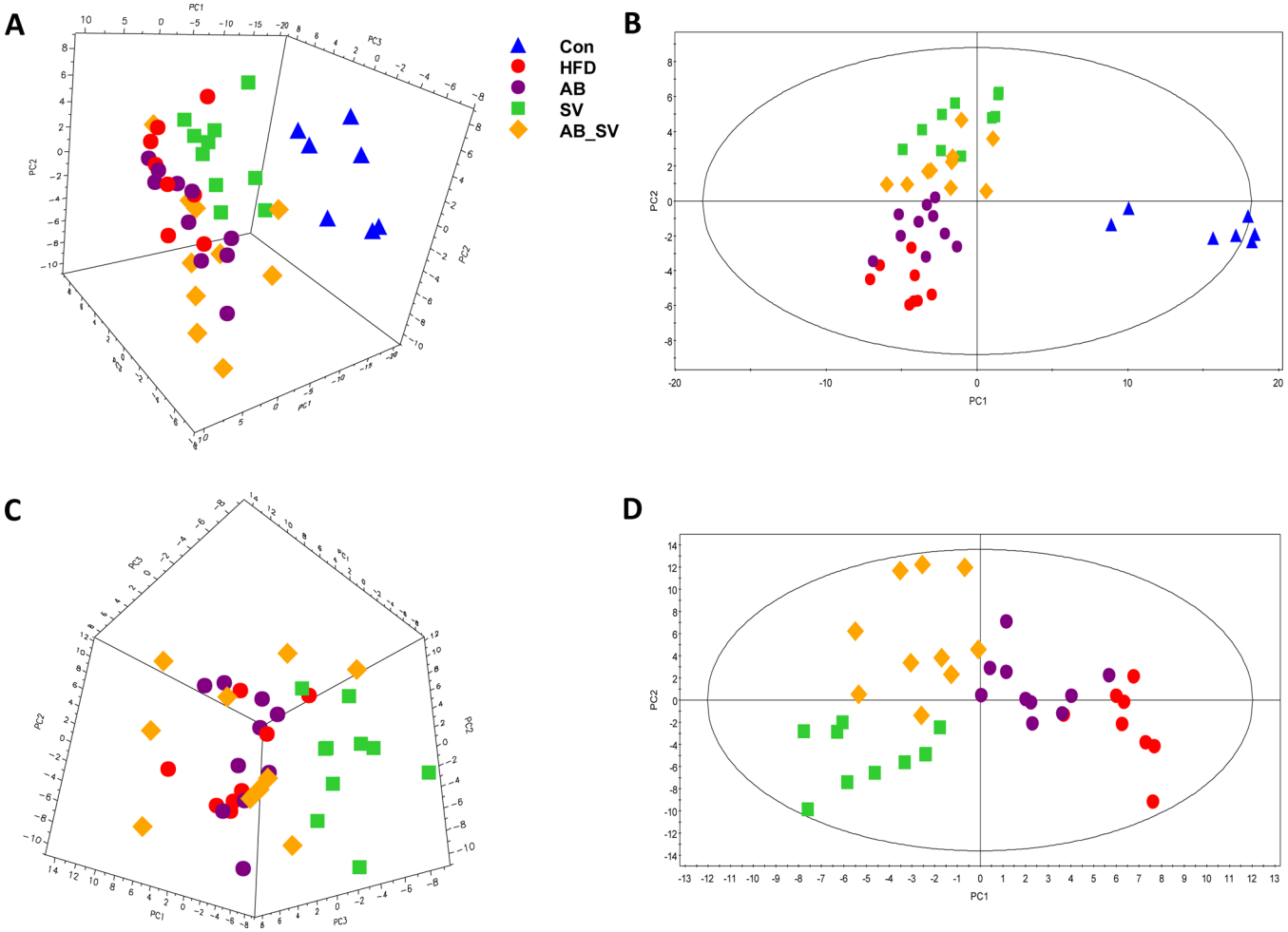

Figure 3. Serum metabolic profiles among groups. (A,B) The 3D PCA score plot and PLS-DA model of all of the five groups based on the identified metabolites in serum with combined GC−MS and UPLC-QTOF-MS. (C,D) The 3D PCA score plot and PLS-DA model of the serum metabolites of the four HFD-fed groups.

DOI: 10.1021/acs.jproteome.6b00984
J. Proteome Res. 2017, 16, 1900−1910

Table 1. Serum Differential Metabolites Based on Combined GC−MS and UPLC-QTOFMS[a]

metabolites	RT_Min	Mz	P-value				fold change (vs Con)			
			HFD vs Con	AB vs HFD	SV vs HFD	AB_SV vs HFD	HFD	AB	SV	AB_SV
MG(20:5)^{LC}	5.12	399.2492	0.000	0.002	0.000	0.001	15.94	10.06	8.55	9.75
Alanine^{GC}	5.66	116	0.002	0.777	0.040	0.563	1.87	1.80	1.38	1.73
LysoPC(16:1)^{LC}	6.8	494.3225	0.000	0.009	0.001	0.000	2.07	1.53	1.40	1.24
LysoPC(18:2)^{LC}	7.06	542.3206	0.000	0.001	0.000	0.000	4.28	3.28	2.80	2.78
LysoPC(18:1)^{LC}	7.55	522.3541	0.000	0.063	0.001	0.001	1.78	1.45	1.17	1.18
MG(18:2)^{LC}	7.58	377.2648	0.000	1.000	0.026	0.629	4.26	3.99	2.86	3.56
PC(36:7)^{LC}	10.11	776.517	0.000	0.553	0.001	0.368	2.62	2.43	1.59	2.35
PC(38:7)^{LC}	10.12	826.5335	0.000	0.263	0.027	0.587	2.30	2.65	1.64	2.46
PC(32:2)^{LC}	10.16	752.5183	0.000	0.989	0.007	0.321	4.85	4.50	2.98	3.77
PC(36:5)^{LC}	10.26	802.5341	0.000	0.300	0.001	0.532	2.14	2.40	1.38	2.00
PE(38:4)^{LC}	10.29	790.5348	0.004	0.596	0.040	0.374	1.99	2.15	1.40	2.25
PC(32:1)^{LC}	10.43	754.5338	0.015	0.447	0.004	0.216	1.49	1.63	0.98	1.28
Glycerol-3-phosphate^{GC}	13.96	357	0.009	0.090	0.026	0.019	1.28	1.12	1.07	1.06
Ribose-5-hosphate^{GC}	17.48	315	0.000	0.521	0.001	0.047	2.41	2.61	1.33	1.79
MG(18:1)^{GC}	22.38	397	0.000	1.000	0.007	0.605	5.23	5.22	2.89	4.34
Cholesterol^{GC}	25.09	329	0.000	1.000	0.000	0.530	2.36	2.29	1.39	2.00

[a]The differential metabolites were determined with the criteria of both VIP > 1 in PLS-DA model of multivariate statistical analysis and $P < 0.05$ in univariate statistical analysis. Fold change was calculated as with the normalized peak intensity.

Gut Microbiota Modulation Altered Serum Metabolic Profile in SV-Treated Mice

To describe the metabolic impacts of gut microbiota modulation on SV-treated mice, serum metabolic profiling was performed by using a combined GC−MS and UPLC-QTOF-MS metabolomic approach. First, the global metabolic profiles were compared with unsupervised PCA, which incorporated the identified 182 serum metabolites (including 99 from GC−MS and 83 from UPLC-QTOF-MS). It showed that samples from the control group were distinctly separated from all the rest of the groups, whereas the HFD and AB groups were almost clustered together. Most samples from the SV and AB_SV groups were clearly separated (Figure 3A). Then, a supervised PLS-DA model was constructed, in which the control group was separated from the rest of the four groups by PC1, while the SV and AB_SV groups were separated from both the HFD and AB groups by PC2 (Figure 3B). The quality of the PCA and PLS-DA models are described in Table S1.

To further characterize the metabolic differences between the SV and AB_SV groups, we constructed a PCA model with the four HFD feeding groups, in which SV group was clearly separated from the rest of the three groups, and the latter three groups were hardly divided (Figure 3C). The following PLS-DA model showed that both the HFD and AB groups were divided from the SV and AB_SV groups by PC1, whereas SV and AB_SV were separated by PC2 (Figure 3D). Accordingly, these results indicated that HFD feeding resulted in transparent alterations in serum metabolic profile, and AB per se did not change it. Moreover, SV treatment dramatically altered the metabolic profile of HFD feeding mice, but not in AB_SV group.

To investigate the metabolic involvement in the therapeutic effect of SV, the key differential metabolites were determined with the criteria of both VIP > 1 in the PLS-DA model and $P < 0.05$ in univariate analysis between control and HFD groups, and were also significantly restored by SV treatment compared to HFD group. A total of 16 key differential metabolites were selected and all of them were increased in the HFD group. The increased differential metabolites in the HFD group mainly belonged to monoglyceride (MG) including MG(18:1), MG(18:2), and MG(20:5); lysophospholipids (LysoPCs) including LysoPC(16:1), LysoPC(18:1), and LysoPC(18:2); phospholipids (PCs) including PC(36:7), PC(38:7), PC(32:2), PC(36:5), and PC(32:1), and phosphatidylethanolamines (PEs) including PE(38:4), as well as cholesterol, glycerol-3-phosphate, alanine, and ribose-5-phosphate. Moreover, most of these metabolites were differently altered in the SV and AB_SV groups, except for the three lysoPCs, MG(20:5), glycerol-3-phosphate, and ribose-5-phosphate that were changed to a similar extent in both the SV and AB_SV groups (Table 1).

In addition to the measurement of serum TC with biochemical kit, we found that the relative concentrations of serum free cholesterol were also significantly increased in the HFD group and greatly reduced in the SV, but not in the AB_SV group as detected by GC−MS. Altogether, the serum metabolic profile indicated that HFD resulted in metabolic alterations, which were effectively restored by SV, but not by AB_SV suggesting the metabolic and gut microbial involvement in mediating the hypolipidemic efficacy of SV.

Gut Microbiota Modulation Altered Serum Bile Acids Profile in SV-Treated Mice

Since bile acids are derived from cholesterol and metabolized by gut microbiota, the variation of serum cholesterol level is associated with the alteration of bile acid metabolism.[21] To investigate the involvement of bile acid metabolism in the hypolipidemic effect of SV with or without gut microbiota modulation, we measured the levels of 16 bile acids in serum samples from different groups with UPLC−MS/MS. The 16 detected bile acids include 7 unconjugated- [cholic acid (CA), chenodeoxycholic acid (CDCA), deoxycholic acid (DCA), lithocholic acid (LCA), α-hyodeoxycholic acid (HDCA), 7-methyldeoxycholic acid (7-MDCA), and ursodeoxycholic acid (UDCA)], five tauro-conjugated- [taurodeoxycholate (TDCA), taurocholic acid (TCA), tauroursodeoxycholic acid (TUDCA), taurohyodeoxycholic acid (THDCA), and taurochenodeoxycholate (TCDCA)] and four glyco-conjugated- [glycoursodeoxycholic acid (GUDCA), glycochenodeoxycholate (GCDCA), glycodeoxycholic acid (GDCA), and glycocholic

DOI: 10.1021/acs.jproteome.6b00984
J. Proteome Res. 2017, 16, 1900−1910

Table 2. Serum Bile Acid Profiles among Groups[a]

bile acids	RT_min	parention (mz)	production (mz)	mean ± SD					fold change (vs Con)			
				Con	HFD	AB	SV	AB_SV	HFD	AB	SV	AB_SV
TUDCA	2.96	498.3	80	0.0443 ± 0.0310	1.5658 ± 0.7962***	2.0043 ± 0.7795***	0.9832 ± 0.2300$^{\#}$	1.7979 ± 0.6881$^{\&}$	35.31	45.20	22.17	40.55
GUDCA	3.04	448.3	74	0.0017 ± 0.0008	0.0032 ± 0.0016*	0.0042 ± 0.0017	0.0029 ± 0.0006	0.0043 ± 0.0026	1.83	2.38	1.67	2.44
THDCA	3.07	498.3	80	0.1073 ± 0.1149	0.1820 ± 0.1491**	0.0886 ± 0.0604	0.1136 ± 0.1324	0.0673 ± 0.0388	1.70	0.83	1.06	0.63
TCA	3.31	514.3	80	1.8730 ± 1.1496	0.5804 ± 0.8325**	0.2201 ± 0.3003	0.1143 ± 0.0730	0.2158 ± 0.1544	0.31	0.12	0.06	0.12
7-MDCA	3.43	405.3	405.3	0.2650 ± 0.1120	2.7288 ± 2.1263***	0.5026 ± 0.2567	0.7531 ± 0.5404$^{\#\#\#}$	0.5790 ± 0.4283	10.30	1.90	2.84	2.18
GCA	3.45	464.3	74	0.0051 ± 0.0020	0.0009 ± 0.0005**	0.0007 ± 0.0002**	0.0009 ± 0.0004	0.0011 ± 0.0006	0.18	0.13	0.17	0.22
TCDCA	3.97	498.3	80	0.1304 ± 0.0545	1.1074 ± 0.5601*	1.1785 ± 0.6343**	0.7467 ± 0.3694	0.8904 ± 0.4683	8.49	9.03	5.72	6.83
UDCA	4.05	391	391	0.0406 ± 0.0108	13.2200 ± 4.3310**	10.8291 ± 3.5748***	8.4961 ± 4.6281$^{\#}$	9.9859 ± 4.6574	325.56	266.68	209.23	245.91
GCDCA	4.13	448.3	74	0.0050 ± 0.0008	0.0052 ± 0.0017	0.0059 ± 0.0012	0.0057 ± 0.0022	0.0065 ± 0.0009	1.03	1.17	1.14	1.29
TDCA	4.15	498.3	80	0.5944 ± 0.1601	0.0408 ± 0.0419***	0.0067 ± 0.0044***	0.0583 ± 0.0866	0.0042 ± 0.0053$^{\&\&\&}$	0.07	0.01	0.10	0.01
HDCA	4.37	391	391	0.0997 ± 0.0883	1.1284 ± 0.6062*	0.4921 ± 0.2995*	0.3741 ± 0.2657$^{\#}$	0.4804 ± 0.2720	11.32	4.94	3.75	4.82
GDCA	4.37	448.3	74	0.0013 ± 0.0009	0.0009 ± 0.0005	0.0010 ± 0.0004	0.0009 ± 0.0004	0.0007 ± 0.0003	0.69	0.79	0.66	0.56
CA	4.61	407.3	407.3	2.8155 ± 0.8031	0.5256 ± 0.1900***	0.4553 ± 0.5534***	0.4928 ± 0.4746	0.9349 ± 0.7786	0.19	0.16	0.18	0.33
CDCA	5.73	391	391	0.0502 ± 0.0203	1.6084 ± 1.1658***	1.0426 ± 0.6028***	0.4810 ± 0.3377$^{\#\#\#}$	1.0630 ± 0.4375$^{\&\&}$	32.06	20.78	9.59	21.19
DCA	5.92	391	391	0.8958 ± 0.3654	0.7226 ± 0.2815	0.4920 ± 0.1678**	0.4138 ± 0.2587$^{\#}$	0.5032 ± 0.2672	0.81	0.55	0.46	0.56
LCA	7.03	375.3	375.3	0.0956 ± 0.0412	0.6162 ± 0.1697***	0.0608 ± 0.0349	1.1976 ± 0.7897	0.0750 ± 0.0410$^{\&\&}$	6.45	0.64	12.53	0.78

[a] *P < 0.05, **P < 0.01, ***P < 0.001 vs Con group; $^{\#}P$ < 0.05, $^{\#\#}P$ < 0.01, $^{\#\#\#}P$ < 0.001 vs HFD group; $^{\&}P$ < 0.05 $^{\&\&}P$ < 0.01, $^{\&\&\&}P$ < 0.001 vs SV group. Comparisons between groups were analyzed with one-way ANOVA followed by a posthoc test. Con: control group; HFD: high-fat/cholesterol diet group; AB: antibiotic group; SV: simvastatin (20 mg/kg) group; AB_SV: simvastatin (20 mg/kg) in the presence of antibiotic treatment.

DOI: 10.1021/acs.jproteome.6b00984
J. Proteome Res. 2017, 16, 1900−1910

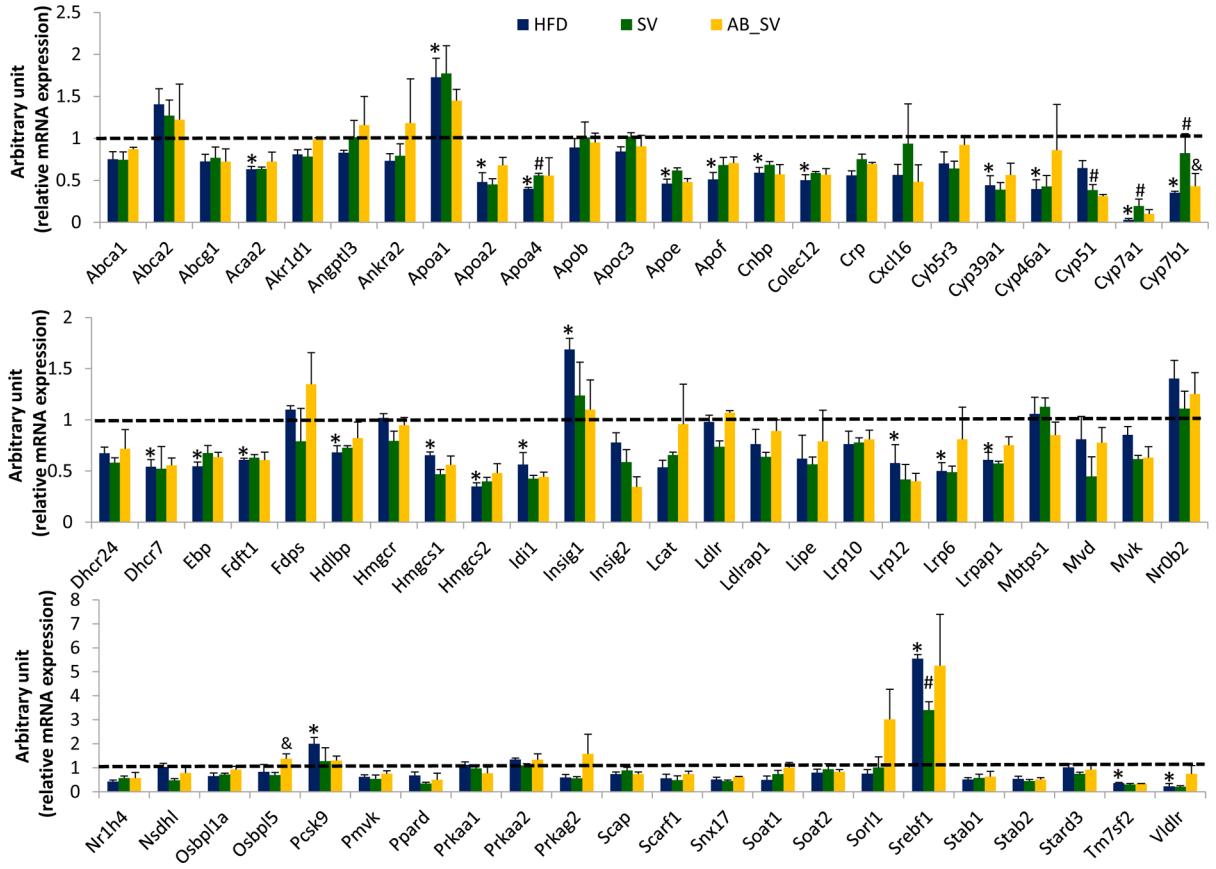

Figure 4. Summary of hepatic gene expression involved in cholesterol metabolism. The expression analysis of genes involved in cholesterol metabolism pathway by using RT2 Profiler Array. Data are means ± SEM of triplicates for each group. $^{*}P < 0.05$ compared to Control group, $^{\#}P < 0.05$ compared to HFD group, $^{\&}P < 0.05$ compared to SV group with one-way ANOVA followed by a posthoc test.

acid (GCA)] bile acids. CA and CDCA are the primary bile acids of mammalian animals. The relative concentrations of CA, TCA and GCA were dramatically reduced in the HFD group compared to the control group, in which only TCA was further depleted by SV treatment. However, gut microbiota modulation did not affect their concentrations either alone or combined with SV. In contrary, increased levels of CDCA and TCDCA were observed in both HFD and AB groups, whereas GCDCA was similar among the 5 groups. TCDCA was deceased either in SV or AB_SV groups to a similar extent; however, CDCA was only reduced by SV treatment, but not AB_SV. UDCA is a kind of hydrophilic bile acid which is used as a cholagogue and choleretic agent in clinic. In our current study, we observed that both UDCA and TUDCA were up-regulated in the HFD and AB groups, and significantly reduced in the SV group, but not in the AB_SV group. LCA is derived from CDCA by gut microbiota. We observed that the relative concentration of LCA was increased in the HFD group, and was further up-regulated in the SV group, but was greatly depleted in either the AB or AB_SV group. In addition, HFD feeding increased the concentration of serum HDCA and 7-MDCA, which were significantly decreased by either SV or AB_SV treatment (Table 2).

Meanwhile, the relative abundance of the detected 16 bile acids was further analyzed. Generally, HFD feeding resulted in obvious changes of detected bile acids in abundance, and minor changes were observed in either the AB or AB_SV group compared to the HFD group. We found that the bile acids in the control group mainly consisted of CA, DCA, TCA, and TDCA, all of which were reduced in the HFD group. The relative abundance of UDCA was over 50% in HFD feeding groups either in the presence of AB, SV or not, while LCA was particularly increased by SV treatment (Figure S1). Altogether, these results indicated that HFD feeding dramatically changed the serum bile acid profiles, which were differently altered in the SV and AB_SV groups.

Expression Analysis of Hepatic Genes in Cholesterol Metabolism Pathways

Given the observed differences in hypolipidemic effect and serum bile acids profile between the SV and AB_SV groups, we wondered whether the differences in hypolipidemic effect between the SV and AB_SV groups were due to the transcriptional regulation of genes involved in cholesterol metabolism pathways. We analyzed the expression of 84 genes that are critically involved in cholesterol metabolism pathway with a commercial RT^2 Profiler PCR Array, among which 14 genes were excluded because of extremely low signaling in all samples. Since AB alone did not affect the levels of serum lipids, the gene expression analysis was specifically focused on samples from the Con, HFD, SV and AB_SV groups. The transcriptional expression of 28 genes was significantly changed by HFD feeding in comparison with the Con group; however, only a very small part of the differently expressed genes were reversed by SV treatment such as Apoa4, Cyp7a1, Cyp7b1, Cyp51 and Srebf1 compared to the HFD group. Among these significantly altered genes, only Cyp7b1 was statistically restored in the AB_SV group compared to the SV group, while Cyp7a1 was

DOI: 10.1021/acs.jproteome.6b00984
J. Proteome Res. 2017, 16, 1900−1910

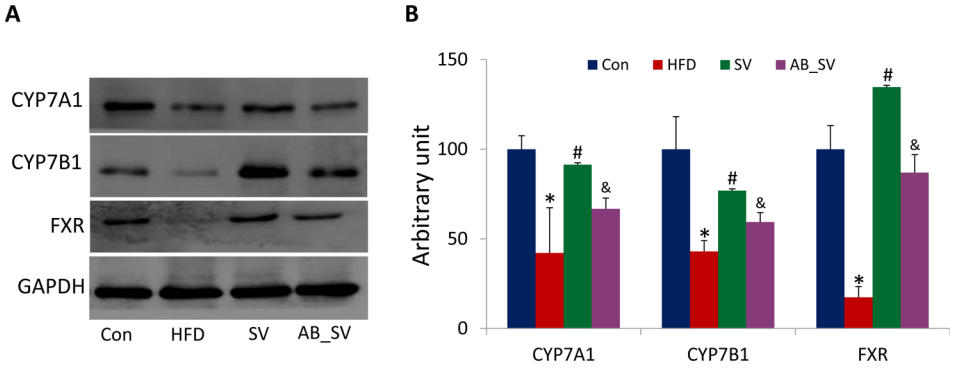

Figure 5. Expression of hepatic proteins with Western blot. (A) The representative bands of hepatic CYP7A1, CYP7B1 and FXR proteins detected with Western blot ($n = 4$). (B) The statistical results of protein expression. Data are means ± SEM. $^{*}P < 0.05$ compared to Control group, $^{\#}P < 0.05$ compared to HFD group, $^{\&}P < 0.05$ compared to SV group with one-way ANOVA followed by a posthoc test.

also restored by AB_SV, but without statistical significance (Figure 4). Therefore, the transcriptional data suggested that the attenuated hypolipidemic effect in the AB_SV group was probably associated with the process of bile acids synthesis.

Gut Microbiota Modulation Decreased SV-Induced Protein Expression in Regulating Bile Acids Synthesis

Given the critical roles of bile acids synthesis in affecting cholesterol level, as well as the observed transcriptional variations of Cyp7a1 and Cyp7b1 genes among different groups, we further measured their expression at the protein level. Our results showed that the expression of these two proteins were significantly down-regulated by HFD feeding. SV treatment significantly up-regulated the expression of both CYP7A1 and CYP7B1 proteins, and this effect was attenuated by gut microbiota modulation (Figure 5A,B). Farnesoid X Receptor (FXR) is one of the intracellular ligand-activated nuclear receptors that plays critical roles in maintaining cholesterol, triglyceride, glucose and bile acid homeostasis.[21] To test whether the attenuated hypolipidemic effect of AB_SV was associated with the regulation on FXR, we measured the expression of FXR protein among groups. We found that HFD feeding resulted in dramatic suppression on FXR protein expression, and was significantly up-regulated in the SV group. However, the SV-induced up-regulation of FXR was attenuated in the AB_SV group (Figure 5A,B). Altogether, our current results indicated that the attenuated hypolipidemic effect of SV by gut microbiota modulation was associated with the suppression of CYP7A1, CYP7B1 and FXR protein expression, which regulate the bile acid synthesis from cholesterol.

DISCUSSION

Our current results showed that gut microbiota modulation by antibiotic could attenuate the hypolipidemic effect of SV in HFD-fed mice, and this effect was accompanied by obvious alterations of serum metabolic and bile acids profiles. Moreover, we found that SV treatment significantly stimulated the expression of hepatic CYP7A1, CYP7B1 and FXR proteins in HFD-fed mice, but was impaired in AB_SV group.

Although genetic factors are important in affecting the efficacy of statins,[22] only a small proportion of the therapeutic variance could be explained by genetic polymorphisms.[23] Recent publications show that different responses to SV therapy correlate with the baseline variations of several kinds of metabolites such as amino acids,[5] phospholipid metabolites[6] and some secondary bacterial-derived bile acids.[7] Meanwhile, SV is metabolized by anaerobic bacteria in human fecal suspension into several SV-derived metabolites step by step.[11] These results highlight the potential involvement of gut microbiota in affecting the hypolipidemic effect of SV. Our results showed that oral administration of antibiotic not only altered the composition of the gut microbiota, but attenuated the hypolipidemic effect of SV as well, demonstrating that different responses to hypolipidemic effect of SV was associated with the differences in gut microbiota. We observed that the bacterial abundance of Gram-positive Firmicutes phylum was greatly reduced, while Gram-negative Proteobacteria phylum was increased by antibiotic administration. Nevertheless, such imbalance between Gram-positive and -negative bacteria in AB-treated mice led to the uncertainty of whether the attenuated lipid-lowering effect of SV was due to the reduced Gram-positive bacteria or the increased Gram-negative bacteria individually or jointly.

Although the metabolic profiles of different responses to SV treatment have been extensively investigated, these studies are mainly focused on identifying differential metabolites either at pre- or postdose of SV treatment that correlate with therapeutic outcomes.[5−7] In our current study, we adopted combined GC−MS and UPLC-QTOF-MS-based metabolomic approach to analyze the metabolic profiles among different groups. Our results indicated that the metabolic profile of SV-treated mice was distinctly different from the rest groups, while this metabolic impact of SV was altered by gut microbiota modulation. Among the identified 16 differential metabolites, some were consistent with the previous observation in human subjects treated with SV. For example, the decreased free cholesterol in current SV-treated mice was also observed in human subjects who were given SV (40 mg/d) for 6 weeks.[5]

Phospholipids PCs and PEs are critical for lipoprotein membrane structure and functions.[24,25] Obvious reduction of PCs and PEs are observed in good responders upon SV treatment.[6] Consistently, our results showed that the increased PCs, PEs, and MGs in HFD group were significantly decreased in SV, but not in AB_SV group, suggesting that gut microbiota modulation altered the metabolism of phospholipids. LysoPCs are formed by hydrolysis of PCs by the enzyme of phospholipase A2,[26] or lecithin:cholesterol acyltransferase (Lcat).[27] The mRNA expression of hepatic Lcat gene was significantly decreased in HFD group, but was similar in both the SV and AB_SV groups. In addition, study indicates SV can inhibit the de novo synthesis of PCs by decreasing phosphocholine cytidylyltransferase activity leading to the

DOI: 10.1021/acs.jproteome.6b00984
J. Proteome Res. 2017, 16, 1900−1910

decrease of plasma lipids.[28] Accordingly, we postulated that gut microbiota modulation might impair the suppression of PCs synthesis by SV in the context of HFD feeding.

Bile acids are derived from cholesterol and cometabolized by gut microbiota.[21] Some bacterial-derived secondary bile acids are predictive for the extent of LDL reduction in SV- treated patients.[7] Therefore, the variations in bile acids metabolism contribute to the different responses to the hypolipidemic effect of SV. Our current results showed that the profile of the 16 analyzed bile acids in serum varied dramatically among groups. LCA is derived from CDCA by intestinal bacteria of Clostridium, a genus of Gram-positive bacteria,[29] which is identified as a marker for good response to SV treatment.[7] We found that the level of LCA was almost doubled in SV group compared to HFD, but maintained at lower concentration in AB and AB_SV groups suggesting that the Clostridium bacteria-derived LCA by HFD feeding was impaired by antibiotic. SV treatment also significantly reduced UDCA and TUDCA in HFD-fed mice; however, the levels of TUDCA were higher in AB_SV group compared to SV group. Although a close association was observed between pretreatment concentrations of UDCA, GUDCA and LDL reduction in SV-treated patients,[7] it was unclear about the roles of reduced UDCA, GUDCA and TUDCA in SV-treated mice. As a result, our results indicated that the attenuated hypolipidemic effect of SV by gut microbiota modulation accompanied by variations of serum bile acids, which implied that the impact of gut microbiota modulation on hypolipidemic effect of SV might be associated with the alterations in bile acids metabolism. CYP7A1 is a critical rate-limiting enzyme for bile acid synthesis from cholesterol that is encoded by Cyp7a1 gene.[30,31] The enhanced enzymatic production of 7-hydroxycholesterol catalyzed by CYP7A1 has been observed in SV-treated macrophages.[32] Our results showed that the expression of hepatic Cyp7a1 gene and its protein was dramatically suppressed by HFD feeding, and greatly stimulated by SV treatment; however, this effect was impaired in AB_SV group. Similar result was also observed in CYP7b1 gene and its protein, which catalyzes the "alternative" pathway of bile acid synthesis.[33] FXR is an important nuclear receptor for regulating bile acid homeostasis via modulation of a series of targeted genes such as Cyp7a1, Cyp8b1, Bsep, Ntcp and so on.[34] On the other hand, FXR can be activated by either free or conjugated bile acids such as CDCA, LCA and DCA. It is observed that mice lacking Fxr gene have elevated LDL and total TG in blood when they are fed with high-cholesterol diet.[35] Moreover, the activation of FXR by agonist or bile acids will lead to reduction of HDL in wide-type mice, and decrease of LDL, HDL and TG in hypercholesterolemia mice.[36] Our current results indicated that hepatic FXR was stimulated by SV in the context of HFD feeding, and this effect was impaired by antibiotic treatment. It is proposed that the diversified actions of statins are due to the activation of FXR;[37] however, little is known about the relationship between the hypolipidemic effect of statins and activation of hepatic FXR so far. Our results revealed that the hypolipidemic effect of SV might be associated with the stimulation of hepatic FXR and FXR-regulated targeted genes, which could be impaired by gut microbiota modulation. Further studies are warranted to investigate the roles of activated hepatic FXR in mediating the hypolipidemic effect of SV, as well as the gut microbial contribution in affecting FXR activation and the downstream biological significance.

■ ASSOCIATED CONTENT

Supporting Information

The Supporting Information is available free of charge on the ACS Publications website at DOI: 10.1021/acs.jproteome.6b00984.

Table S1, Summary of the PCA and PLS-DA Models; Figure S1, The relative abundance of detected serum bile acids among groups (PDF)

■ AUTHOR INFORMATION

Corresponding Authors

*E-mail: wjia@cc.hawaii.edu.
*E-mail: houkai1976@126.com. Tel: +86-021-5132-2748.

ORCID

Houkai Li: 0000-0003-2846-7895

Author Contributions

#X.H., N.Z., and J.H. contributed equally.

Notes

The authors declare no competing financial interest.
The sequence information on 16S rDNA from fecal samples has been uploaded to the Sequence Read Archive database under the accession number SRP093219.

■ ACKNOWLEDGMENTS

We would like to thank Dr. Xianfu Gao (Shanghai Prof Leader Biotech Co, Ltd) for his assistance with the metabolomic analysis. This work was financially supported by Shanghai Pujiang Program (14PJD031) from the Science and Technology Commission of Shanghai Municipality, Shanghai Creative Research Fund (ZYX-CXYJ-017) of Higher Education, Program for Professor of Special Appointment (Eastern Scholar) at Shanghai Institutions of Higher Learning from Shanghai Municipal Education Commission, and National Natural Science Foundation of China (No. 81673662).

■ REFERENCES

(1) Grundy, S. M.; Cleeman, J. I.; Merz, C. N.; Brewer, H. B., Jr.; Clark, L. T.; Hunninghake, D. B.; Pasternak, R. C.; Smith, S. C., Jr.; Stone, N. J.; National Heart, L.; Blood, I.; American College of Cardiology, F.; American Heart, A.. Implications of recent clinical trials for the National Cholesterol Education Program Adult Treatment Panel III guidelines. *Circulation* **2004**, *110*, 227−239.

(2) Zhou, Z.; Rahme, E.; Pilote, L. Are statins created equal? Evidence from randomized trials of pravastatin, simvastatin, and atorvastatin for cardiovascular disease prevention. *Am. Heart J.* **2006**, *151*, 273−281.

(3) Baigent, C.; Keech, A.; Kearney, P. M.; Blackwell, L.; Buck, G.; Pollicino, C.; Kirby, A.; Sourjina, T.; Peto, R.; Collins, R.; Simes, R. Cholesterol Treatment Trialists, C. Efficacy and safety of cholesterol-lowering treatment: prospective meta-analysis of data from 90,056 participants in 14 randomised trials of statins. *Lancet* **2005**, *366*, 1267−1278.

(4) Simon, J. A.; Lin, F.; Hulley, S. B.; Blanche, P. J.; Waters, D.; Shiboski, S.; Rotter, J. I.; Nickerson, D. A.; Yang, H.; Saad, M.; Krauss, R. M. Phenotypic predictors of response to simvastatin therapy among African-Americans and Caucasians: the Cholesterol and Pharmacogenetics (CAP) Study. *Am. J. Cardiol.* **2006**, *97*, 843−850.

(5) Trupp, M.; Zhu, H.; Wikoff, W. R.; Baillie, R. A.; Zeng, Z. B.; Karp, P. D.; Fiehn, O.; Krauss, R. M.; Kaddurah-Daouk, R. Metabolomics reveals amino acids contribute to variation in response to simvastatin treatment. *PLoS One* **2012**, *7*, e38386.

DOI: 10.1021/acs.jproteome.6b00984
J. Proteome Res. 2017, 16, 1900−1910

(6) Kaddurah-Daouk, R.; Baillie, R. A.; Zhu, H.; Zeng, Z. B.; Wiest, M. M.; Nguyen, U. T.; Watkins, S. M.; Krauss, R. M. Lipidomic analysis of variation in response to simvastatin in the Cholesterol and Pharmacogenetics Study. *Metabolomics* **2010**, *6*, 191−201.
(7) Kaddurah-Daouk, R.; Baillie, R. A.; Zhu, H.; Zeng, Z. B.; Wiest, M. M.; Nguyen, U. T.; Wojnoonski, K.; Watkins, S. M.; Trupp, M.; Krauss, R. M. Enteric microbiome metabolites correlate with response to simvastatin treatment. *PLoS One* **2011**, *6*, e25482.
(8) Nicholson, J. K.; Holmes, E.; Kinross, J.; Burcelin, R.; Gibson, G.; Jia, W.; Pettersson, S. Host-gut microbiota metabolic interactions. *Science* **2012**, *336*, 1262−1267.
(9) Li, H.; He, J.; Jia, W. The influence of gut microbiota on drug metabolism and toxicity. *Expert Opin. Drug Metab. Toxicol.* **2016**, *12*, 31−40.
(10) Kim, D. H. Gut Microbiota-Mediated Drug-Antibiotic Interactions. *Drug Metab. Dispos.* **2015**, *43*, 1581−1589.
(11) Aura, A. M.; Mattila, I.; Hyotylainen, T.; Gopalacharyulu, P.; Bounsaythip, C.; Oresic, M.; Oksman-Caldentey, K. M. Drug metabolome of the simvastatin formed by human intestinal microbiota in vitro. *Mol. BioSyst.* **2011**, *7*, 437−446.
(12) Yoo, D. H.; Kim, I. S.; Van Le, T. K.; Jung, I. H.; Yoo, H. H.; Kim, D. H. Gut microbiota-mediated drug interactions between lovastatin and antibiotics. *Drug Metab. Dispos.* **2014**, *42*, 1508−1513.
(13) Zheng, X. J.; Zhao, A. H.; Xie, G. X.; Chi, Y.; Zhao, L. J.; Li, H. K.; Wang, C. R.; Bao, Y. Q.; Jia, W. P.; Luther, M.; Su, M. M.; Nicholson, J. K.; Jia, W. Melamine-Induced Renal Toxicity Is Mediated by the Gut Microbiota. *Sci. Transl. Med.* **2013**, *5*, 172ra122−172ra122.
(14) Zhang, X.; Zhao, Y.; Zhang, M.; Pang, X.; Xu, J.; Kang, C.; Li, M.; Zhang, C.; Zhang, Z.; Zhang, Y.; Li, X.; Ning, G.; Zhao, L. Structural changes of gut microbiota during berberine-mediated prevention of obesity and insulin resistance in high-fat diet-fed rats. *PLoS One* **2012**, *7*, e42529.
(15) DeSantis, T. Z.; Hugenholtz, P.; Larsen, N.; Rojas, M.; Brodie, E. L.; Keller, K.; Huber, T.; Dalevi, D.; Hu, P.; Andersen, G. L. Greengenes, a chimera-checked 16S rRNA gene database and workbench compatible with ARB. *Appl. Environ. Microbiol.* **2006**, *72*, 5069−5072.
(16) Ludwig, W.; Strunk, O.; Westram, R.; Richter, L.; Meier, H.; Yadhukumar; Buchner, A.; Lai, T.; Steppi, S.; Jobb, G.; Forster, W.; Brettske, I.; Gerber, S.; Ginhart, A. W.; Gross, O.; Grumann, S.; Hermann, S.; Jost, R.; Konig, A.; Liss, T.; Lussmann, R.; May, M.; Nonhoff, B.; Reichel, B.; Strehlow, R.; Stamatakis, A.; Stuckmann, N.; Vilbig, A.; Lenke, M.; Ludwig, T.; Bode, A.; Schleifer, K. H. ARB: a software environment for sequence data. *Nucleic Acids Res.* **2004**, *32*, 1363−1371.
(17) Schloss, P. D.; Westcott, S. L.; Ryabin, T.; Hall, J. R.; Hartmann, M.; Hollister, E. B.; Lesniewski, R. A.; Oakley, B. B.; Parks, D. H.; Robinson, C. J.; Sahl, J. W.; Stres, B.; Thallinger, G. G.; Van Horn, D. J.; Weber, C. F. Introducing mothur: open-source, platform-independent, community-supported software for describing and comparing microbial communities. *Appl. Environ. Microbiol.* **2009**, *75*, 7537−7541.
(18) Cole, J. R.; Wang, Q.; Cardenas, E.; Fish, J.; Chai, B.; Farris, R. J.; Kulam-Syed-Mohideen, A. S.; McGarrell, D. M.; Marsh, T.; Garrity, G. M.; Tiedje, J. M. The Ribosomal Database Project: improved alignments and new tools for rRNA analysis. *Nucleic Acids Res.* **2009**, *37*, D141−145.
(19) Caporaso, J. G.; Kuczynski, J.; Stombaugh, J.; Bittinger, K.; Bushman, F. D.; Costello, E. K.; Fierer, N.; Pena, A. G.; Goodrich, J. K.; Gordon, J. I.; Huttley, G. A.; Kelley, S. T.; Knights, D.; Koenig, J. E.; Ley, R. E.; Lozupone, C. A.; McDonald, D.; Muegge, B. D.; Pirrung, M.; Reeder, J.; Sevinsky, J. R.; Turnbaugh, P. J.; Walters, W. A.; Widmann, J.; Yatsunenko, T.; Zaneveld, J.; Knight, R. QIIME allows analysis of high-throughput community sequencing data. *Nat. Methods* **2010**, *7*, 335−336.
(20) Gao, X.; Pujos-Guillot, E.; Sebedio, J. L. Development of a quantitative metabolomic approach to study clinical human fecal water metabolome based on trimethylsilylation derivatization and GC−MS analysis. *Anal. Chem.* **2010**, *82*, 6447−6456.
(21) Li, T.; Chiang, J. Y. Bile acid signaling in metabolic disease and drug therapy. *Pharmacol. Rev.* **2014**, *66*, 948−983.
(22) Barber, M. J.; Mangravite, L. M.; Hyde, C. L.; Chasman, D. I.; Smith, J. D.; McCarty, C. A.; Li, X.; Wilke, R. A.; Rieder, M. J.; Williams, P. T.; Ridker, P. M.; Chatterjee, A.; Rotter, J. I.; Nickerson, D. A.; Stephens, M.; Krauss, R. M. Genome-wide association of lipid-lowering response to statins in combined study populations. *PLoS One* **2010**, *5*, e9763.
(23) Mangravite, L. M.; Wilke, R. A.; Zhang, J.; Krauss, R. M. Pharmacogenomics of statin response. *Curr. Opin Mol. Ther.* **2008**, *10*, 555−561.
(24) Lagace, T. A.; Ridgway, N. D. The role of phospholipids in the biological activity and structure of the endoplasmic reticulum. *Biochim. Biophys. Acta, Mol. Cell Res.* **2013**, *1833*, 2499−2510.
(25) Sweeney, G.; Nazir, D.; Clarke, C.; Goettsche, G. Ethanolamine and choline phospholipids in nascent very-low-density lipoprotein particles. *Clin. Invest. Med.* **1996**, *19*, 243−250.
(26) Carlquist, J. F.; Muhlestein, J. B.; Anderson, J. L. Lipoprotein-associated phospholipase A2: a new biomarker for cardiovascular risk assessment and potential therapeutic target. *Expert Rev. Mol. Diagn.* **2007**, *7*, 511−517.
(27) Soupene, E.; Borja, M. S.; Borda, M.; Larkin, S. K.; Kuypers, F. A. Featured Article: Alterations of lecithin cholesterol acyltransferase activity and apolipoprotein A-I functionality in human sickle blood. *Exp. Biol. Med. (London, U. K.)* **2016**, *241*, 1933−1942.
(28) Yanagita, T.; Yamamoto, K.; Ishida, S.; Sonda, K.; Morito, F.; Saku, K.; Sakai, T. Effects of simvastatin, a cholesterol synthesis inhibitor, on phosphatidylcholine synthesis in HepG2 cells. *Clin. Ther.* **1994**, *16*, 200−208.
(29) Houten, S. M.; Watanabe, M.; Auwerx, J. Endocrine functions of bile acids. *EMBO J.* **2006**, *25*, 1419−1425.
(30) Chiang, J. Y. Bile acids: regulation of synthesis. *J. Lipid Res.* **2009**, *50*, 1955−1966.
(31) Cohen, J. C.; Cali, J. J.; Jelinek, D. F.; Mehrabian, M.; Sparkes, R. S.; Lusis, A. J.; Russell, D. W.; Hobbs, H. H. Cloning of the human cholesterol 7 alpha-hydroxylase gene (CYP7) and localization to chromosome 8q11-q12. *Genomics* **1992**, *14*, 153−161.
(32) Xu, X.; Zhang, A.; Halquist, M. S.; Yuan, X.; Henderson, S. C.; Dewey, W. L.; Li, P. L.; Li, N.; Zhang, F. Simvastatin promotes NPC1-mediated free cholesterol efflux from lysosomes through CYP7A1/LXRalpha signalling pathway in oxLDL-loaded macrophages. *J. Cell Mol. Med.* **2017**, *21*, 364.
(33) Ren, S.; Marques, D.; Redford, K.; Hylemon, P. B.; Gil, G.; Vlahcevic, Z. R.; Pandak, W. M. Regulation of oxysterol 7alpha-hydroxylase (CYP7B1) in the rat. *Metab., Clin. Exp.* **2003**, *52*, 636−642.
(34) Claudel, T.; Staels, B.; Kuipers, F. The Farnesoid X receptor: a molecular link between bile acid and lipid and glucose metabolism. *Arterioscler., Thromb., Vasc. Biol.* **2005**, *25*, 2020−2030.
(35) Sinal, C. J.; Tohkin, M.; Miyata, M.; Ward, J. M.; Lambert, G.; Gonzalez, F. J. Targeted disruption of the nuclear receptor FXR/BAR impairs bile acid and lipid homeostasis. *Cell* **2000**, *102*, 731−744.
(36) Zhang, Y.; Lee, F. Y.; Barrera, G.; Lee, H.; Vales, C.; Gonzalez, F. J.; Willson, T. M.; Edwards, P. A. Activation of the nuclear receptor FXR improves hyperglycemia and hyperlipidemia in diabetic mice. *Proc. Natl. Acad. Sci. U. S. A.* **2006**, *103*, 1006−1011.
(37) Howe, K.; Sanat, F.; Thumser, A. E.; Coleman, T.; Plant, N. The statin class of HMG-CoA reductase inhibitors demonstrate differential activation of the nuclear receptors PXR, CAR and FXR, as well as their downstream target genes. *Xenobiotica* **2011**, *41*, 519−529.

DOI: 10.1021/acs.jproteome.6b00984
J. Proteome Res. 2017, 16, 1900−1910